

A spectral-spatial pulse for improved signal recovery in the small-tip fast recovery (STFR) sequence

Sydney N Williams¹, Hao Sun², Jon-Fredrik Nielsen¹, Jeffrey A Fessler², and Douglas C Noll¹

¹Biomedical Engineering, University of Michigan, Ann Arbor, Michigan, United States, ²Electrical Engineering, University of Michigan, Ann Arbor, Michigan, United States

Target Audience: RF engineers and MR physicists interested in signal loss recovery for steady-state sequences.

Introduction: A new method for RF pulse design is proposed with improved signal loss recovery for balanced steady-state imaging. Recently, spin echo formation using phase pre-winding has been proposed to correct for weak dephasing of spin isochromats less than 2π [1]. In [2] this pre-winding RF pulse was used with the new “small-tip fast recovery” (STFR) sequence [3,4] to achieve steady-state imaging with similar image contrast as balanced steady-state free precession (bSSFP) but with potential for reduced banding and other artifacts. In [2], STFR RF pulses were designed spectrally, where the pre-winding phase bandwidth is selected a priori based on the off-resonance distribution. However, there are bandwidth constraints for a pure spectral design that limit its benefit for the STFR sequence [1]. In this work, we improve upon the spectral design pattern with a 2D spectral-spatial pulse, varying the target phase pattern spatially based on voxel-by-voxel off-resonance. This pulse leverages the effective bandwidth of the design pattern, improving the signal recovery in inhomogeneous objects imaged with STFR.

Pulse Design: The STFR sequence is comprised of four steps: (1) A tip-down RF pulse is applied, (2) the spins freely precess for a given readout time T_{free} accumulating phase θ , (3) a tip-up RF pulse brings the spin isochromats back towards the longitudinal direction, and (4) a gradient crusher dephases the remaining transverse magnetization [4]. We designed both RF pulses by iteratively solving the regularized weighted least squares problem $\hat{b} = \text{argmin}_b \|Ab - d\|_w^2 + \beta \|b\|_2^2$ presented in [5]. Here, b is the RF pulse waveform, d is the target magnetization pattern, and A is the MR signal system matrix for the small-tip regime given by $a_{i,j} = i\gamma M_0 e^{2\pi i(\mathcal{F}(i) \cdot \mathbf{k}(j))} \Delta t$. We define γ as the gyromagnetic ratio, Δt the sampling period, \mathcal{F} a stack of three column vectors containing samples at resonant frequency and 2 spatial locations (x,y) , and \mathbf{k} a stack of three row vectors with the reversed time samples of the pulse and 2 excitation k-space trajectories (k_x, k_y) . For the tip-down pulse, the target design pattern is set to be $d = \sin(\alpha) e^{2\pi i j \frac{T_{\text{free}}}{2}}$ for flip angle α , and target phase bandwidth f which is some portion of the entire frequency range contained within a measured B_0 field map. The frequency range of f varies for each spatial location, and is centered at the field map off-resonance value. For the tip-up pulse, we use a similar target design technique where the magnetization phase is estimated from a simulation of the isochromats behavior at the end of the free precession interval, and a negative field map is used in the design. Furthermore, the pulse is time-reversed and negated to bring the spins back up towards the longitudinal direction [3]. To encode the spatial off-resonance information within the pulse design, we used a uniform density spiral k-space trajectory that repeated for 3 cycles over the RF pulse. A 3ms RF pulse was designed with $\alpha = 5^\circ$, $f = 150\text{Hz}$, and $T_{\text{free}} = 3.7\text{ms}$. The pulse was regularized to control for integrated power (SAR) and peak RF hardware constraints. Fig. 1 shows the 2D spectral-spatial pulse and gradient waveforms.

Experimental Methods: We imaged a healthy volunteer using a 3T GE scanner with birdcage head coil. A 3D field map was acquired and a 2D slice was selected for design where the total off-resonance difference across the slice was approximately 150Hz. The field map was then used to design the spectral-spatial RF pulse as well as a purely spectral tip-down, tip-up pulse scheme [2]. The STFR sequence was used with both pulse schemes to image the subject with a $64 \times 64 \times 64$ gradient echo readout with $\text{FOV} = 24 \times 24 \times 32 \text{cm}$. The 2D slice that was chosen for the design was used to compare the performance of the spectral-spatial and purely spectral designs.

Results: Fig. 2 shows the field map slice used for the RF pulse designs, the simulated residual magnetization of the signal after Bloch simulation of the entire pulse sequence, and the reconstructed images of the slice. In Fig. 2b,c the normalized residual magnetization is lower for the spectral-spatial pulse design method, 0.013 vs. 0.016 for purely spectral. For Fig. 2d,e there is higher signal recovery for the proposed method at the inhomogeneous region of the brain near the sinus cavities (mean signal intensity of ROI is 0.21 for spectral-spatial, 0.14 for purely spectral). Furthermore, by taking the Euclidean norm of the two pulses as surrogate for SAR, the spectral-spatial pulse reduced the integrated power by 27% for the tip-down pulse and 23% for the tip-up pulse compared to the purely spectral pulse.

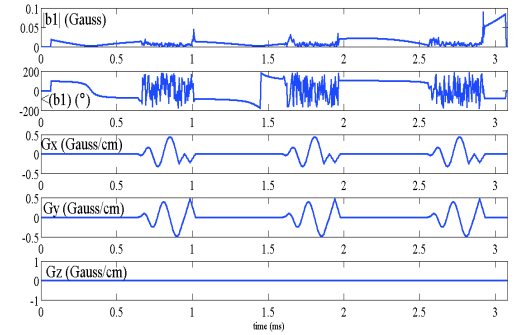


Figure 1. RF pulse b , and gradient trajectories G_x , G_y , and G_z for the tip-down pulse of the STFR sequence. The tip-up pulse is similar in appearance yet time-reversed

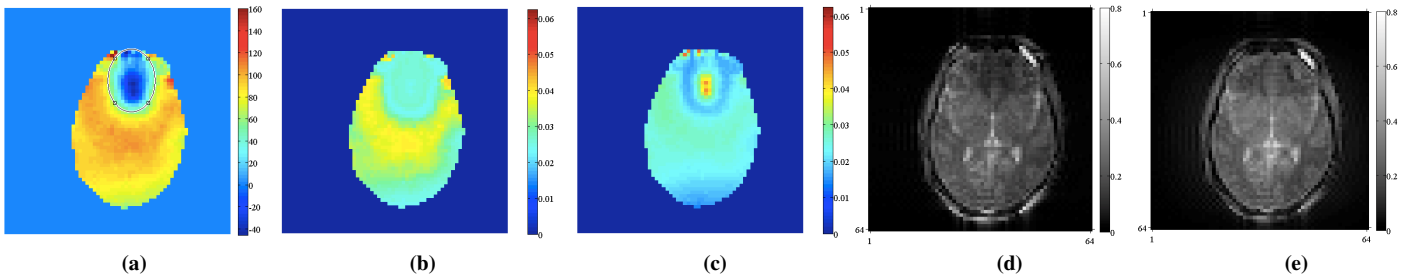


Figure 2. (a) Field map of slice used for pulse design with ROI ellipse drawn around area of signal inhomogeneity near sinus cavities. (b,c) Residual magnetization prior to tip-up pulse based on Bloch simulation of purely spectral (b) and spectral-spatial pulse (c). (d,e) Reconstructed images acquired with the STFR sequence for purely spectral (d) and spectral-spatial pulse (e) designs. The spectral-spatial pulse design method has enhanced signal recovery in the ellipse ROI shown in (a).

Conclusion: We developed a method for incorporating spatially varying off-resonance information from a field map into a spectral pre-winding phase pattern. This allowed for a 2D spectral-spatial pulse that exhibited better signal recovery for the STFR sequence than a purely spectral RF pulse. Furthermore, the relative integrated power of the spectral-spatial pulse was lower than the purely spectral pulse, reducing SAR during the image acquisition. In the future, we will adapt the pulse design method for 3D spectral-spatial pulses. We will also investigate methods for automating the regularization needed to solve the weighted least squares problem for various k-space trajectories. We expect that additional work will enhance the effective bandwidth of off-resonance so that we can recover signal over widely varying 3D volumes.

[1] Asslander et al., ISMRM 2014 [2] Sun et al., ISMRM 2014 [3] Nielsen et al., MRM 2013 [4] Sun et al., MRM 2014 [5] Yip et al., MRM 2005.